Periodica Polytechnica Electrical Engineering and Computer Science, 67(3), pp. 281–290, 2023

Practical Automatic Tuning of Lag-lead Compensators for Feedback Control Systems

Yu-Sheng Lu[1*], Tsang-Shiuan Tsai[1], Chin-Hao Lai[2]

[1] Department of Mechatronic Engineering, National Taiwan Normal University, 162 Heping E. Road, 106 Taipei, Taiwan
[2] Department of Mechanical Engineering, National Yunlin University of Science and Technology, 123 University Road, 64002 Yunlin, Taiwan
[*] Corresponding author, e-mail: luys@ntnu.edu.tw

Received: 16 November 2022, Accepted: 01 February 2023, Published online: 28 March 2023

Abstract

This paper proposes a scheme for auto-tuning a lag-lead compensator to satisfy frequency-domain specifications of a feedback control system. Most previous studies proposed algorithms for tuning either lag or lead compensators. A study presented a self-tuning lag-lead compensator whose proportional gain, however, needs to be set manually. In contrast to previous studies, a fully automated tuning process for a lag-lead compensator is devised in this paper. In the proposed scheme, the plant's frequency responses at specific frequencies are first estimated, and an iterative algorithm adapts all controller parameters. To facilitate the estimation of high loop gain at a low frequency, a notch filter is introduced to the control loop while estimating this high low-frequency loop gain. Without this mechanism, a real-time data acquisition system of a wide dynamic range would be required. In addition to fulfilling the requirements for the low-frequency loop gain and phase margin, another feature of the proposed scheme is the satisfaction of the required gain-crossover frequency. However, the proposed method supposes that the frequency-domain specifications can be met for a plant using a lag-lead compensator, which is the plant's requirement for the proposed method. Experimental results for controlling a voice-coil motor are reported in this paper, showing that the proposed auto-tuner can practically provide a lag-lead compensated system satisfying frequency-domain performance requirements.

Keywords

automatic tuning, control system, frequency-domain specification, lag-lead compensator, loop gain, stability margin

1 Introduction

The lag-lead compensator and the proportional-integral-derivative (PID) controller are the two most important categories of feedback controllers in practical applications. Owing to its convenient form and simple implementation, the PID controller is widely used for industrial automation processes [1], where the processes to be controlled are also referred to as plants in the context of control system engineering. Designing a PID controller often requires a plant's mathematical model that is always either uncertain or unknown, and there is a need to automatically tune controller parameters, which attracts a lot of research efforts. The most well-known heuristic tuning guidelines for the PID controller are the Ziegler-Nichols rules [2], which do not require prior knowledge of a plant's mathematical model to determine three controller gains. These are the gains of proportional, integral, and derivative control terms. In the Ziegler-Nichols rules, the ultimate-cycle method uses only a proportional controller, adjusts the proportional gain to produce persistent oscillations in the plant's output, and records the corresponding proportional gain and oscillation period respectively referred to as the ultimate gain and period. The ultimate gain and period are then used to determine the PID gains. Rather than bringing about a risk of closed-loop instability during the tuning process, the relay feedback test [3] and its modifications [4–7] were proposed to automatically measure the ultimate gain and period. Many other tuning algorithms have also been proposed based on the iterative feedback tuning method [8], pole-compensation method [9], frequency-domain approach [10, 11], or internal model control structure [12]. Heuristic search algorithms, such as genetic algorithm [13] and artificial bee colony optimization algorithm [14], have been applied to determine PID gains. Besides, fuzzy logic and artificial neural networks are used to mimic or online

Cite this article as: Lu, Y.-S., Tsai, T.-S., Lai, C.-H. "Practical Automatic Tuning of Lag-lead Compensators for Feedback Control Systems", Periodica Polytechnica Electrical Engineering and Computer Science, 67(3), pp. 281–290, 2023. https://doi.org/10.3311/PPee.21533

tune the PID controller [15, 16], being an emerging area of control technologies.

A lag-lead compensator has been applied to control a lot of physical systems, such as an optical image stabilization system [17], a head-positioning control system in a disk drive [18], and a power system [19]. Compared with the PID controller, the lag-lead compensator can provide high-frequency attenuation, thus reducing sensitivity to high-frequency measurement noise and unmodeled dynamics. Due to limited low-frequency gain, it also alleviates the so-called integrator-windup phenomenon that is commonly encountered in a PID-controlled system. The lag-lead compensator that aggregates both lag and lead compensators is an improved form of the PID controller [20]. However, the tuning of a lag-lead compensator involves more parameters and thus more complex algorithms than that of the PID controller. Previous works on the auto-tuning of a lag-lead compensator are much less than those on the PID auto-tuning. For integrating processes, Tsang et al. [21] proposed a method for auto-tuning a lead compensator, in which a specification for relative stability is given in terms of phase margin. The studies [20–23] proposed algorithms for tuning either a lag or a lead compensator, rather than a complete lag-lead compensator. Nassirharand [24] developed a self-tuning lag-lead compensator, in which a proportional gain needs to be set manually.

The frequency-domain method is reliable and practical for control system applications [25]. Based on the frequency response technique, this study develops a fully automated tuning process for a lag-lead compensator that consists of a lag compensator for adequate low-frequency loop gain and a lead compensator for sufficient relative stability. Unlike the study [24], the proposed tuning process does not require manually setting a proportional gain for the lag-lead compensator. In contrast to the previous studies, there are two additional salient features of the proposed scheme. One is the achievement of online estimation of a high low-frequency gain, which would require a real-time signal processing system of a wide dynamic range without using the proposed scheme. The other feature is the fulfillment of requirements not only on the phase margin but also on the gain-crossover frequency. An experimental study is conducted for a voice coil motor of a disk drive. The rest of this paper is arranged as follows. First, an experimental system and performance specifications in the frequency domain are presented. Second, how to estimate frequency responses of the plant at specific frequencies is explained. Third, an iterative algorithm for auto-tuning a lag-lead compensator is proposed. Lastly, experimental results are reported, and conclusions are provided.

2 An experimental system with performance specifications

Consider a focus system of an optical disk drive, in which a voice coil motor drives an objective lens. This servo system is to concentrate a laser beam onto an information layer of an optical disk by actively adjusting the position of the objective lens. However, due to disk wobbles, the rotation of a disk causes persistent movements of the data layer, and the focus servo needs enough low-frequency loop gain, bandwidth, and relative stability to continually move the lens and regulate the focal point as close to the information layer as possible.

The focusing error should be within ± 0.23 μm whereas the maximum allowable disk wobble is ± 0.3 mm, requiring a minimum loop gain of 1300 or, equivalently, 62.3 dB. According to the DVD (Digital Versatile Disc) physical specifications for read-only disk, the loop gain should be between 66 and 86 dB from 9.6 to 23.1 Hz. Hence, the specification for the low-frequency loop gain is set to 76 dB at 25 Hz. Moreover, according to the DVD physical specifications for read-only disk, the maximum allowable acceleration of the disk wobble is 8 m/s^2, giving the specification of at least 2000 Hz for a gain-crossover frequency. In the DVD physical specifications for read-only disk, there is no specification for the phase margin. The phase margin for the focus system is generally required to be greater than 35 degrees based on experience in industrial practice. The specification for the phase margin is chosen to be 40 degrees in this paper. The performance requirements for the focus system are summarized as follows:

1. a low-frequency loop gain of 66 dB at the frequency of 25 Hz;
2. a gain-crossover frequency of at least 2000 Hz;
3. a phase margin of 40 degrees.

In some literature, the gain-crossover frequency is also referred to as the unity-gain frequency. Fig. 1 shows a block diagram of the focus system, where r denotes the reference, $P(s)$ denotes the plant's unknown transfer function, u is the plant's input, and $C(s)$ represents a focus controller that is a lag-lead compensator. In this system, the measurable signal for feedback is the output error, e_o, and the distance between the lens and the disk's information layer is

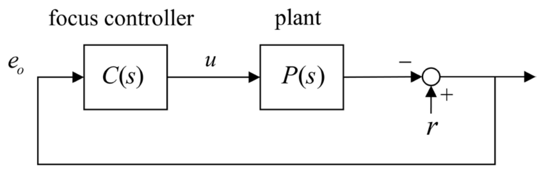

Fig. 1 Block diagram of the focus servo system in normal operation

kept constant by regulating e_o to zero. That is, when $e_o = 0$, this distance almost equals the focal length. The lag-lead compensator has Eq. (1):

$$C(s) = K_l \frac{s+\beta\omega_l}{\beta(s+\omega_l)} \times \frac{\alpha\left(s+\omega_g/\sqrt{\alpha}\right)}{s+\sqrt{\alpha}\omega_g}, \tag{1}$$

in which $\omega_l = 2\pi \times 25$, and K_l, β, α and ω_g are controller parameters to be auto-tuned. Fig. 2 shows the asymptotic magnitude Bode plot for the lag-lead compensator, in which K_g denotes the gain at the frequency of ω_g, and K_m denotes the constant gain in the frequency range of $\beta\omega_l$ and $\omega_g/\sqrt{\alpha}$. It is worth noting that the asymptote between ω_l and $\beta\omega_l$ is given by $K_l\omega_l/s$ whereas the asymptote between $\omega_g/\sqrt{\alpha}$ and $\sqrt{\alpha}\omega_g$ is described by $K_g s/\omega_g$. It is desired to devise an auto-tuning law to decide the controller parameters, K_l, β, α and ω_g, for satisfying the performance requirements.

3 Estimation of frequency responses at specific frequencies

Auto-tuning a compensator needs information on the plant [26]. In practice, the plant's transfer function, $P(s)$, is either uncertain or unknown. Implementation of a general self-tuning controller involves setting up a mathematical model for the plant as well as online identification of the model's parameters using a system identifier, which is a demanding task. Rather than performing complete modeling and identification of the plant, this paper presents an approach that online measures frequency responses of the plant only at some specific frequencies that are required for satisfying the performance requirements. This is done by injecting exogenous sinusoidal signals of specific frequencies into the control loop and estimating corresponding frequency responses.

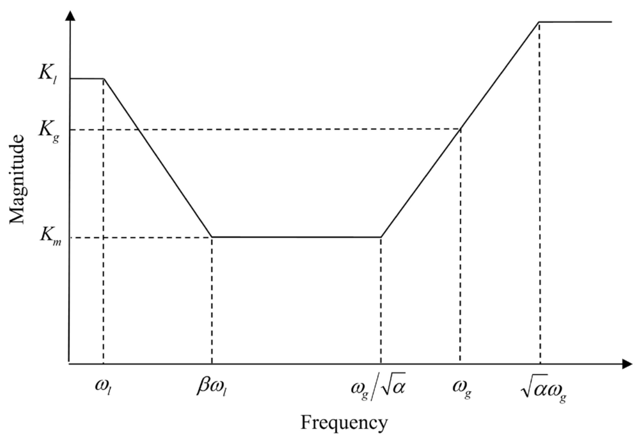

Fig. 2 Asymptotic magnitude Bode plot for the lag-lead compensator

Fig. 3 shows the block diagram for estimating frequency responses at specific frequencies, in which a sinusoidal signal having an amplitude of K_r is introduced to the control loop, and e_s equals e_o plus that sinusoid. The sinusoidal signal, the controller, the bandpass filter, and Fourier analyses, shown in Fig. 3, are realized using a DSP (digital signal processor). Fourier analyses are employed to find the loop gain by calculating Fourier coefficients of e_o:

$$a_o = \frac{2}{NT}\int_0^{NT} e_o \cos\omega t \, dt, \tag{2}$$

$$b_o = \frac{2}{NT}\int_0^{NT} e_o \sin\omega t \, dt, \tag{3}$$

and those of e_s:

$$a_s = \frac{2}{NT}\int_0^{NT} e_s \cos\omega t \, dt, \tag{4}$$

$$b_s = \frac{2}{NT}\int_0^{NT} e_s \sin\omega t \, dt, \tag{5}$$

in which ω equals either ω_l or ω_g, $T = 2\pi/\omega$ and a natural number, N, denotes the number of cycles of the sinusoid used to perform Fourier analyses. Through gain and phase calculations, the loop gain at the frequency of ω is obtained as:

$$C(j\omega)G(j\omega) = \frac{\sqrt{a_o^2+b_o^2}}{\sqrt{a_s^2+b_s^2}} \angle\left(\tan^{-1}\frac{a_o}{b_o} - \tan^{-1}\frac{a_s}{b_s}\right), \tag{6}$$

in which $G(s)$ equals either $P(s)$ or $P(s)$ in cascade with a notch filter. As shown in Fig. 3, the notch filter is implemented as $1 + H(s)$, in which $H(s)$ is a bandpass filter described by:

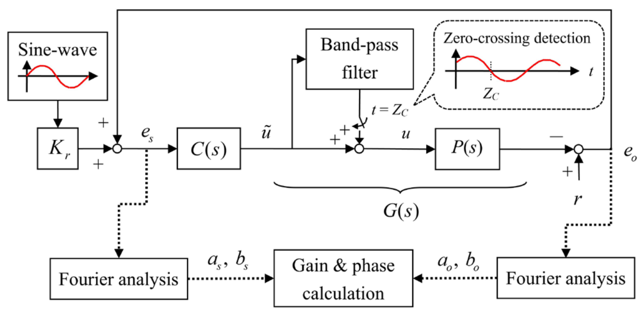

Fig. 3 Estimation of frequency responses at specific frequencies

$$H(s) = \frac{2(\zeta - 0.707)\omega_l s}{s^2 + 2\times 0.707\omega_l s + \omega_l^2}. \quad (7)$$

The parameter, ζ, in Eq. (7) is used to determine the magnitude of attenuation of the notch filter at ω_l. The notch filter has a Butterworth polynomial of order 2 and provides a gain of $\zeta/0.707$ at the frequency of ω_l. In normal operation or when measuring the frequency response at ω_g, the switch shown in Fig. 3 is open, and the notch filter is ineffective. The notch filter is active only when estimating the frequency response at ω_l. Because the loop gain at the low frequency, ω_l, is rather high, making the magnitude of e_s extremely small relative to that of e_o. To reduce the difference between the dynamic ranges of e_s and e_o for stable implementation, the auto-tuner incorporates the notch filter into the control loop while estimating the frequency response at ω_l. Moreover, to have a bumpless transfer, a zero-crossing detection mechanism is implemented, which makes the notch filter become effective once there is a zero-crossing in the output of the bandpass filter, $H(s)$. In this study, ζ is selected to let the filter have an attenuation of 46 dB at ω_l. Using Eq. (6), the loop gains at ω_l and ω_g can be obtained; that is, $C(j\omega_l)G(j\omega_l)$ and $C(j\omega_g)G(j\omega_g)$ can be estimated. Moreover, since the frequency responses of $C(s)$ and $H(s)$ are known, the plant's gains, $P(j\omega)$ with ω equal to ω_l and ω_g, can be evaluated, enabling subsequent tuning procedures.

4 Iterative auto-tuning of a lag-lead compensator

The control system needs to have a low-frequency loop gain of 66 dB at 25 Hz so ω_l is fixed to $2\pi \times 25$ rad/s. On the other hand, the system requires a unity-gain frequency of at least 2000 Hz so ω_g is initially set to $2\pi \times 2000$ rad/s. Once the auto-tuner completes the evaluation of $P(j\omega_l)$ and $P(j\omega_g)$, the following tuning process is commenced:

1. *Step 1.* (*Determination of* K_l): since the loop gain at ω_l requires 66 dB, the low-frequency gain of the lag-lead compensator is given by letting:

   $$K_l = D_t \big/ \left|P(j\omega_l)\right|, \quad (8)$$

   in which the desired loop gain $D_t = 10^{(66+3)/20} = 10^{69/20}$.
2. *Step 2.* (*Determination of* K_g *and* α): as shown in Fig. 2, the compensator gain at ω_g is denoted as K_g. This gain should be chosen to have ω_g be the gain-crossover frequency, giving:

   $$K_g = \left|P(j\omega_g)\right|^{-1}. \quad (9)$$

   To obtain a desired phase margin of 40 degrees, the phase that needs to be provided by the lead compensation is initially set to $\phi = -140° - \angle P(j\omega_g)$, which is then used to decide the parameter:

   $$\alpha = \frac{1+\sin\phi}{1-\sin\phi}. \quad (10)$$
3. *Step 3.* (*Determination of* K_m *and* β): the gain, K_m, can be decided from the lead part of the compensator. As shown in Fig. 2, the asymptote between $\omega_g/\sqrt{\alpha}$ and $\sqrt{\alpha}\omega_g$ is described by $K_g s/\omega_g$. The gain, K_m, is the magnitude of this asymptote at the frequency of $\omega_g/\sqrt{\alpha}$, giving:

   $$K_m = \left|K_g s/\omega_g\right|_{s=j\omega_g/\sqrt{\alpha}} = K_g/\sqrt{\alpha}, \quad (11)$$

   in which K_g and α have been determined in *Step 2*. To decide β, consider the asymptote between ω_l and $\beta\omega_l$, which is described by $K_l\omega_l/s$. As shown in Fig. 2, the magnitude of this asymptote at the frequency of $\beta\omega_l$ equals K_m, leading to:

   $$K_m = \left|K_l\omega_l/s\right|_{s=j\beta\omega_l} = K_l/\beta. \quad (12)$$

   Equating Eqs. (11) and (12) gives:

   $$\beta = \sqrt{\alpha}K_l/K_g, \quad (13)$$

   in which K_l is specified in *Step 1*, and K_g and α are given in *Step 2*.
4. *Step 4.* (*Examination and iteration*): so far, a prototype of the lag-lead compensator has been decided. Subsequently, the phase margin of the resulting system is examined. If the phase margin is unsatisfactory, then increase the nominal phase lead, ϕ, by 1°, and redo from *Step 2* until the phase margin cannot be further increased by increasing ϕ. When the phase margin cannot be improved by increasing ϕ, then increase ω_g by 200 Hz, estimate $P(j\omega_g)$, and redo from *Step 2*. If the phase margin is satisfactory, then the auto-tuning process is terminated. This so-obtained analog compensator is then digitized using the bilinear transformation with prewarping of the gain-crossover frequency, ω_g, and the compensator parameters are updated.

Fig. 4 illustrates the flow chart of the auto-tuning algorithm, in which PM denotes the phase margin. The proposed auto-tuning algorithm yields a lag-lead compensator's

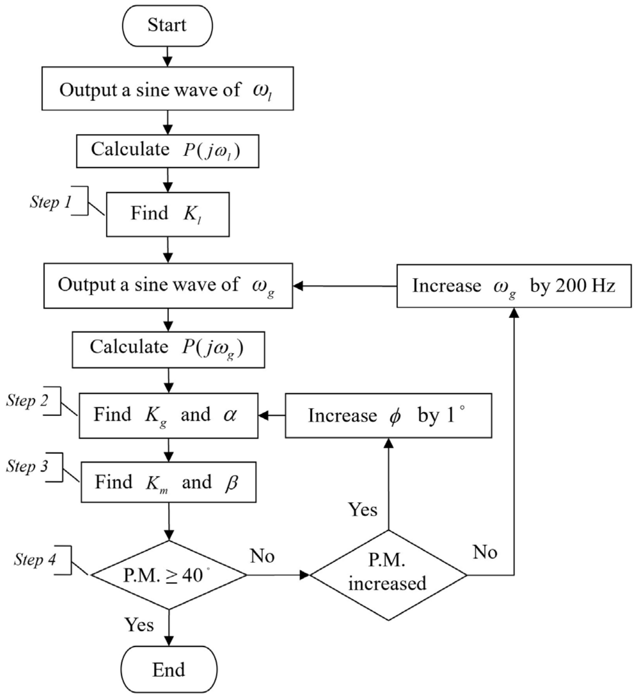

Fig. 4 Flow chart of the auto-tuning process

parameters using the reasoning based on an asymptotic magnitude Bode plot, which approximates an actual Bode plot. When the parameter, β, of the compensator's lag part is large, the phase lead by the compensator can diminish and become smaller than expected, giving an unsatisfactory phase margin. As shown in Fig. 4, when the phase margin is insufficient, the nominal phase lead, ϕ, is increased by 1° per iteration. Furthermore, if the phase margin cannot be improved by increasing ϕ, then ω_g is increased by 200 Hz per iteration.

The proposed method supposes that the frequency-domain specifications can be met for a plant using a lag-lead compensator, which is the plant's requirement for the proposed method. Specifically, the proposed method is applicable to minimum-phase plants with a relative degree of two or fewer. Note that the frequency-domain specifications considered in this paper include a required gain-crossover frequency. When a plant has a relative degree higher than two, a high required gain-crossover frequency implies that the specifications cannot be all satisfied using a lag-lead compensator, demanding the use of multi-stage lead compensation or specification relaxation. With the validity of the assumption that the specifications can be met using a lag-lead compensator, the auto-tuning process, shown in Fig. 4, can converge. When this assumption cannot be ensured, the auto-tuning process should be amended with an additional exit condition.

5 Experimental study

5.1 Realization of the auto-tuner

The control system is realized using DSP/FPGA (field-programmable gate array) hardware. The FPGA handles the timing of all input-output peripherals and sends an external interrupt request signal to the DSP. After receiving this interrupt request, the DSP commences an interrupt service routine to execute the algorithms for the auto-tuner and the compensator. The clock speed of the FPGA is 100 MHz. This clock is divided by 2^9, producing an interrupt request signal of 195.3125 kHz to the DSP. Hence, the sampling frequency of the DSP is 195.3125 kHz.

With this sampling frequency, practical ω_l is set to $2\pi \times 25.0016$ rad/s, and the initial ω_g is approximated to $2\pi \times 1992.9846$ rad/s. Table 1 lists parameters for estimating $P(j\omega_l)$ and $P(j\omega_g)$, where δ denotes a tolerance boundary of gain estimation in percentage, and ψ is a parameter to determine whether the system has entered a steady state for stable gain estimation after being subject to an injected sinusoid. In the proposed algorithm, $P(j\omega)$, $\omega = \omega_l$ or ω_g, is estimated every N cycles of the injected sinusoid with an amplitude of K_r. Let $P_i(j\omega)$ denote the i-th estimate of $P(j\omega)$ for $\omega = \omega_l$ or ω_g. If the relation, $\left|1 - P_{i-1}(j\omega)/P_i(j\omega)\right| \le \delta/100$, is valid for ψ consecutive times, then the current estimate, $P_i(j\omega)$, is considered a valid estimate of $P(j\omega)$. Once $P(j\omega_l)$ and $P(j\omega_g)$ are estimated, the DSP automatically starts finding parameters of the lag-lead compensator using the algorithm described in Section 4.

5.2 Results from different initial controllers

The plant was identified, giving a nominal transfer function of $1.065 \times 10^8/(s^2 + 39.82\,s + 4.119 \times 10^5)$ for designing initial controllers. This nominal transfer function reveals that the plant has a damping ratio of 0.03 and a natural frequency of 642 rad/s. Unlike a general DC motor, the plant does not include an integrator and has a pair of lightly damped dominant poles. Because of the lag compensation, an integrating effect is not required in the controller. Based on the plant's nominal model, two initial controllers are chosen using the trial-and-error method. The two initial controllers, $C_A(s)$ and $C_B(s)$, are respectively described by:

Table 1 Parameters for evaluating $P(j\omega_l)$ and $P(j\omega_g)$

	K_r (V)	N (cycles)	δ (%)	ψ (times)	Notch filter introduced?
For $P(j\omega_l)$	0.2	5	20	15	Yes
For $P(j\omega_g)$	0.1	1	2	15	No

$$C_A(s) = \frac{2.498\ s^2 + 1.475\times10^4 s + 1.221\times10^7}{6.34\ s^2 + 2.036\times10^5 s + 3.182\times10^7}, \tag{14}$$

$$C_B(s) = \frac{110.6\ s^2 + 1.095\times10^6 s + 2.711\times10^9}{31.65\ s^2 + 1.012\times10^6 s + 1.582\times10^8}, \tag{15}$$

in which $C_A(s)$ has less low-frequency gain than $C_B(s)$. The low-frequency loop gains with $C_A(s)$ and $C_B(s)$ are respectively 37.3 and 70.2 dB at 25 Hz, being respectively lower and higher than the specification of 66 dB. On the other hand, the nominal phase margins with $C_A(s)$ and $C_B(s)$ are both less than the specification of 40 degrees. These initial compensators were intentionally detuned to verify if the auto-tuner could modify the compensators to meet the specifications. With a disk's rotational frequency of 1200 rpm, Fig. 5 shows signals during an auto-tuning process with the initial controller, $C_A(s)$, in which a pull-in detection signal, *PI*, indicates if the laser beam is focused onto the information layer of an optical disk. Moreover, to indicate status of the DSP controller, a single-bit flag, *Flag*, is toggled whenever the DSP initiates a different task. As shown in Fig. 5, when the DSP has the focus servo on, the *PI* goes high, revealing that the laser spot has been nearly focused on the information layer. After the *PI* remains high for some time, the focus status is designated as *Focus OK*, which allows the auto-tuner to first estimate $P(j\omega_g)$ with ω_g near 2.0 kHz. Subsequently, the auto-tuner estimates $P(j\omega_l)$ and starts an iteration process for finding compensator parameters. When the desired phase margin is unattainable with ω_g near 2.0 kHz, then ω_g is increased to near 2.2 kHz, and the auto-tuner estimates $P(j\omega_g)$ and continues the iteration process further. As shown in Fig. 5, the auto-tuner finally decides compensator parameters with ω_g near 2.2 kHz and updates the lag-lead compensator for normal operation. Fig. 6 shows the evolution of phase margin during the tuning process. It is seen that the phase margin is initially increasing with respect to the number of iterations. However, the phase margin obtained at the 18th iteration becomes smaller than that obtained at the 17th iteration, so the auto-tuner increases ω_g to near 2.2 kHz and continues the iteration process. As shown in Fig. 6, the desired phase margin is achieved at the 27th iteration.

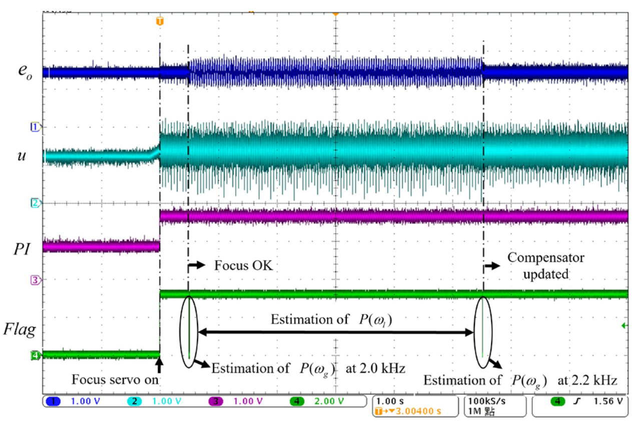

Fig. 5 Auto-tuning process with the initial controller, $C_A(s)$

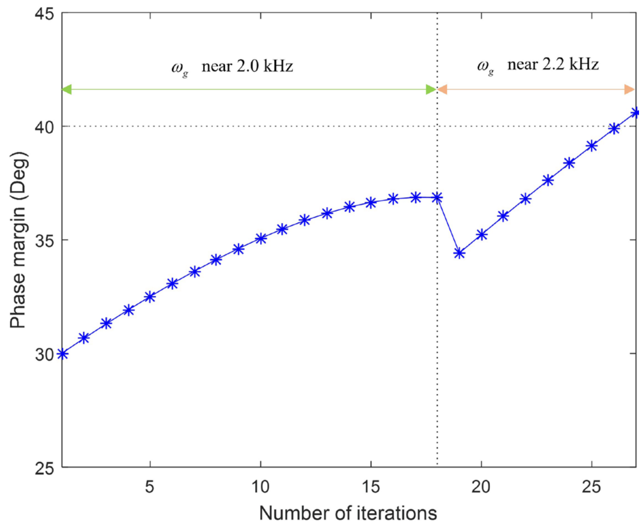

Fig. 6 Evolution of phase margin during the tuning process

Fig. 7 shows the loop gains before and after auto-adjustment using the preliminary compensators, $C_A(s)$ and $C_B(s)$, in which these loop gains are obtained using a sound-and-vibration module, PXI 4461, National Instruments. It is seen that these loop gains with $C_A(s)$ and $C_B(s)$ are quite different and do not fulfill the required specifications. After auto-adjustment, the loop gains become close to each other. Table 2 lists performance indices after auto-tuning using different initial controllers. It is seen that although the initial controllers are distinct, both auto-tuned systems have performance indices close to the desired specifications.

5.3 Results for systems subject to large disturbances

Another disk drive is used in the following experiments to examine the same auto-tuner with another physical plant. Besides, a disk with a wobble of ± 0.5 mm from Teac Corporation is used to test the auto-tuner with significant disturbances due to the rotation of this wobbling disk. Fig. 8 shows auto-tuning results of two experiments with the same initial controller, $C_A(s)$, but with two different rotational speeds of the disk, 1200 and 2400 rpm. It is seen that the tuning results are satisfactory despite significant disk wobbles. However, with a disk's rotational speed of 1200 rpm, there are fluctuations in the measured loop gains at 20 and 40 Hz respectively corresponding to one and two times the disk's rotational frequency. Since

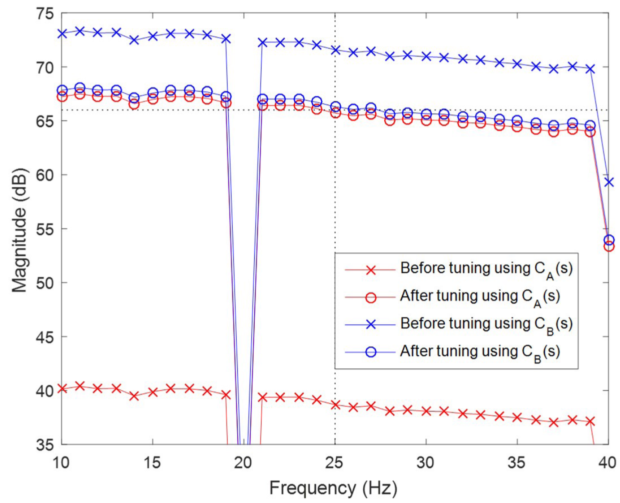

(a)

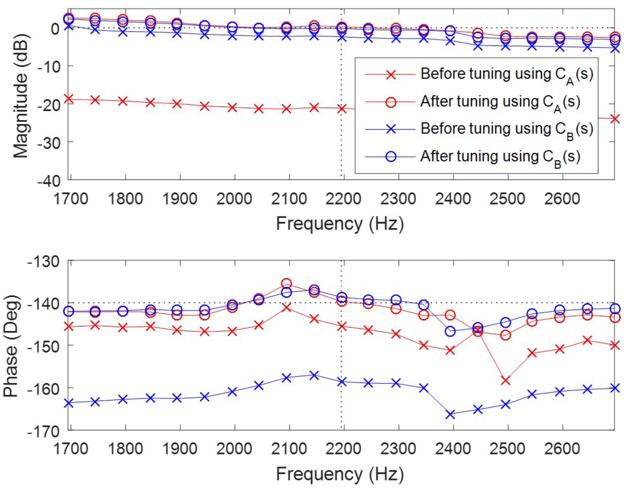

(b)

Fig. 7 Auto-tuning results with different initial controllers; (a) around 25 Hz; (b) around the gain-crossover frequency

Table 2 Auto-tuning results with different initial controllers

	Gain at ω_l (dB)	Gain at ω_g (dB)	P.M. (°)
With the initial controller, $C_A(s)$	65.713	0.253	40.321
With the initial controller, $C_B(s)$	66.301	−0.486	41.297

the interested frequency of the auto-tuner is 25 Hz, these disturbances at 20 and 40 Hz do not noticeably influence the auto-tuning of low-frequency loop gain. Moreover, as shown in Fig. 8, doubling the disk's rotational speed to 2400 rpm does not have much influence on auto-tuning.

Fig. 9 shows the time response of the focus servo system before and after auto-tuning at the disk's rotational speed of 2400 rpm. It is seen that before the auto-adjustment, the output error, e_o, is excessive and much affected

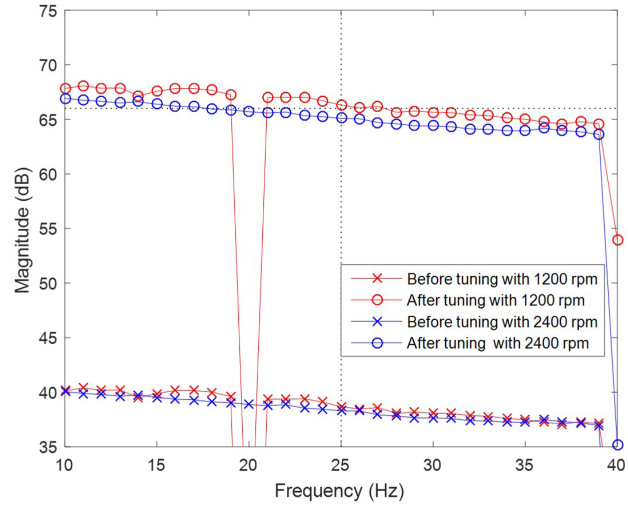

(a)

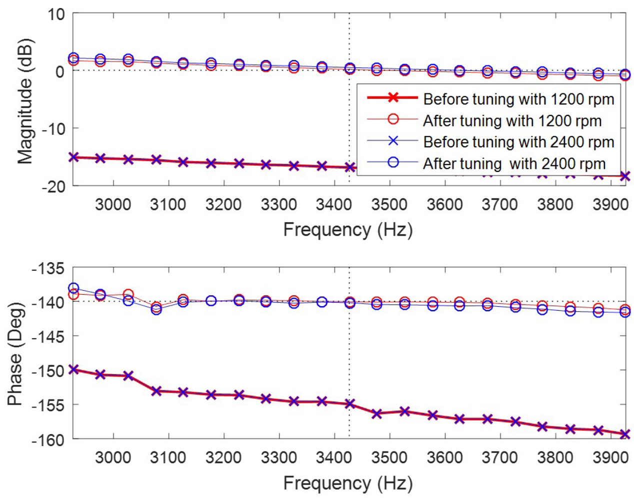

(b)

Fig. 8 Auto-tuning results with a wobbling disk; (a) around 25 Hz; (b) around the gain-crossover frequency

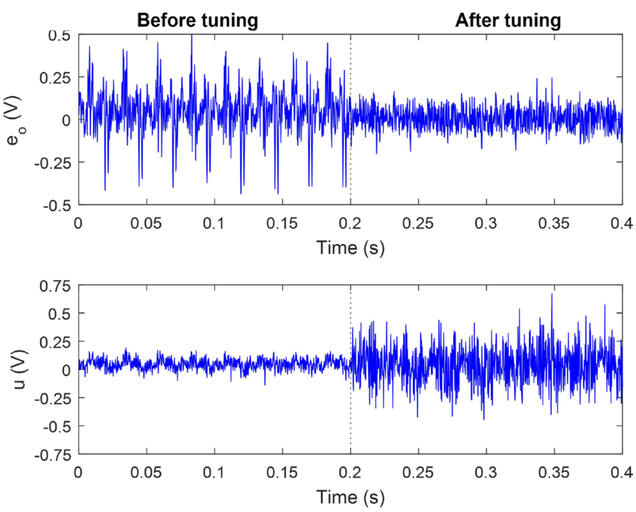

Fig. 9 Dynamic responses before and after adjustment with a wobbling disk

by disk wobbles. After the auto-tuning, the output error is greatly alleviated, implying that the lag-lead compensator has been well tuned. Table 3 shows the performance indices of the auto-tuned system with the wobbling disk at different rotational speeds. In these experiments, the gain-crossover frequency, ω_g, is automatically adjusted to near 3.4 kHz, and the performance indices after tuning are close to the aforementioned requirements. These results show that the proposed auto-tuner can be robust to unknown disturbances and also to the variation of the disk's rotational speed.

5.4 Experimental results for systems with substantial noises

In the following experiments, the wobbling disk is replaced by another test disk also from Teac Corporation. Onto this test disk, black-band defects were deliberately introduced. When the laser spot is within the zone of black band, almost no light will be reflected from the disk, so valid feedback signals will vanish. In this situation, there exist substantial noises in the feedback signals. Fig. 10 shows the auto-tuning process with a black-band disk using the initial controller, $C_A(s)$. Compared with the *PI* signal shown in Fig. 5, the *PI* signal shown in Fig. 10 can abruptly drop down for short periods due to black-band defects. It is also seen from the *Flag* signal shown in Fig. 10 that the auto-tuner increases ω_g several times to meet the requirement of phase margin. Fig. 11 shows the evolution of phase margin during the tuning process. It is seen that whenever the phase margin cannot be further increased at a specific ω_g, the auto-tuner increases ω_g by 200 Hz until the desired phase margin is attained. In this experiment, ω_g is successively increased to near 3.4 kHz, and the phase margin is automatically tuned to reach 40 degrees.

Fig. 12 shows the auto-tuning results with a black-band disk using two initial controllers, $C_A(s)$ and $C_B(s)$. Here, initial low-frequency loop gains are either lower or higher than necessary, and initial phase margins are all lower than required. Despite the black-band defects, both auto-tuned systems have loop gains close to the specifications. Table 4 lists the resulting performance indices. It demonstrates that the gains at ω_l and ω_g are respectively close to 66 and 0 dB with ω_g greater than 2.0 kHz. Moreover, the resulting phase margins are approximately 40 degrees. It demonstrates that the auto-tuner is able to deal with noises induced by black-band defects.

Table 3 Auto-tuning results with a wobbling disk at different rotational speeds

	Gain at ω_l (dB)	Gain at ω_g (dB)	P.M. (°)
Wobbling disk at 1200 rpm	66.295	0.163	39.961
Wobbling disk at 2400 rpm	65.091	0.496	39.812

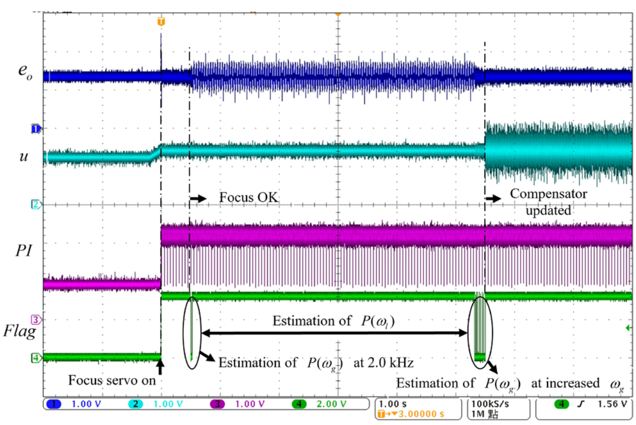

Fig. 10 Auto-tuning with a black-band disk using the initial controller, $C_A(s)$

6 Conclusion

This paper presents a scheme for auto-tuning a lag-lead compensator to satisfy frequency-domain requirements. In the proposed scheme, sinusoidal signals of specific frequencies are injected into the feedback system, and the plant's frequency responses at these specific frequencies are estimated. Especially, a notch filter is implemented as a unity gain in parallel with a band-pass filter and is used to enable stable estimation of high loop gain at a low frequency. Based on the concept of asymptotic Bode diagram, an auto-tuning algorithm is proposed to

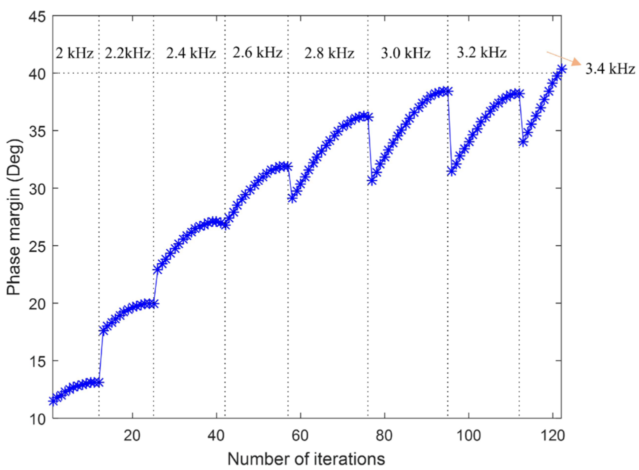

Fig. 11 Evolution of phase margin during the tuning process

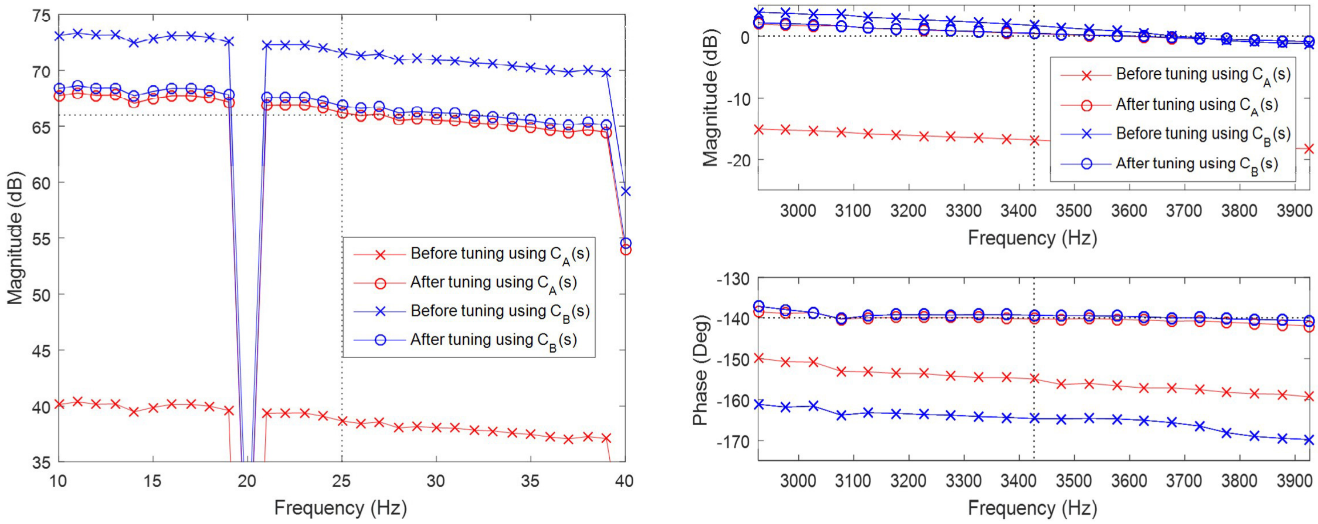

(a)

(b)

Fig. 12 Auto-tuning results with a black-band disk; (a) around 25 Hz; (b) around the gain-crossover frequency

Table 4 Auto-tuning results with a black-band disk

	Gain at ω_l (dB)	Gain at ω_g (dB)	P.M. (°)
With the initial controller, $C_A(s)$	66.208	0.394	39.679
With the initial controller, $C_B(s)$	66.853	−0.486	40.601

iteratively adjust all compensator parameters for fulfilling the requirements on both the phase margin and the gain-crossover frequency. Experimental studies on the voice coil motor of a disk drive have been conducted. Experimental results show that the auto-tuned system can meet the performance specifications despite using different initial controllers, the existence of substantial disturbances, and corruption of feedback signals. These experimental results demonstrate the feasibility and practicality of the proposed auto-tuning scheme.

Acknowledgement
The authors are grateful to the financial support of the National Science and Technology Council, Taiwan, through grant MOST 111-2221-E-003-028.

References

[1] Kiong, T. K., Qing-Guo, W., Chien, H. C., Hägglund, T. J. "Advances in PID control", Springer, 1999. ISBN 978-1-4471-1219-8 https://doi.org/10.1007/978-1-4471-0861-0

[2] Ziegler, J. G., Nichols N. B. "Optimum setting for automatic controllers", Transactions of the ASME, 64(8), pp. 759–768, 1942. https://doi.org/10.1115/1.4019264

[3] Åström, K. J., Hägglund, T. "Automatic tuning of simple regulators with specifications on phase and amplitude margins", Automatica, 20(5), pp. 645–651, 1984. https://doi.org/10.1016/0005-1098(84)90014-1

[4] Lee, T. H., Wang, Q. G., Tan, K. K. "A modified relay-based technique for improved critical point estimation in process control", IEEE Transactions on Control Systems Technology, 3(3), pp. 330–337, 1995. https://doi.org/10.1109/87.406980

[5] Sung, S. W., Park, J. H., Lee, I.-B. "Modified relay feedback method", Industrial & Engineering Chemistry Research, 34(11), pp. 4133–4135, 1995. https://doi.org/10.1021/ie00038a059

[6] Tan, K. K., Lee, T. H., Wang, Q. G. "Enhanced automatic tuning procedure for process control of PI/PID controllers", AIChE Journal, 42(9), pp. 2555–2562, 1996. https://doi.org/10.1002/aic.690420916

[7] Shen, S.-H., Yu, H.-D., Yu, C.-C. "Use of saturation-relay feedback for autotune identification", Chemical Engineering Science, 51(8), pp. 1187–1198, 1996. https://doi.org/10.1016/0009-2509(95)00371-1

[8] Lequin, O., Gevers, M., Mossberg, M., Bosmans, E., Triest, L. "Iterative feedback tuning of PID parameters: comparison with classical tuning rules", Control Engineering Practice, 11(9), pp. 1023–1033, 2003. https://doi.org/10.1016/S0967-0661(02)00303-9

[9] Hamida, M. L., Fekik, A., Denoun, H., Kadi, F. "Experimental identification and control of a 3kW DC motor", Periodica Polytechnica Electrical Engineering and Computer Science, 66(4), pp. 301–314, 2022. https://doi.org/10.3311/PPee.20421

[10] Nyitrai, A., Szabó, G., Horváth, S. R. "Parameter determination and drive control analysis of axial flux permanent magnet synchronous motors", Periodica Polytechnica Electrical Engineering and Computer Science, 66(2), pp. 205–214, 2022. https://doi.org/10.3311/PPee.19714

[11] Lu, Y.-S., Tsai, T.-S., Huang, C.-C., Cheng, C.-H. "PID auto-tuning for simultaneously fulfilling the requirements of relative stability and steady-state error", Artificial Life and Robotics, 26(2), pp. 162–168, 2021. https://doi.org/10.1007/s10015-020-00661-z

[12] Castellanos-Cárdenas, D., Castrillón, F., Vásquez, R. E., Smith, C. "PID tuning method based on IMC for inverse-response second-order plus dead time processes", Processes, 8(9), 1183, 2020. https://doi.org/10.3390/pr8091183

[13] Feng, H., Yin, C.-B., Weng, W.-W., Ma, W., Zhou, J.-J., Jia, W.-H., Zhang, Z.-L. "Robotic excavator trajectory control using an improved GA based PID controller", Mechanical Systems and Signal Processing, 105, pp. 153–168, 2018. https://doi.org/10.1016/j.ymssp.2017.12.014

[14] Du, H., Liu, P., Cui, Q., Ma, X., Wang, H. "PID controller parameter optimized by reformative artificial bee colony algorithm", Journal of Mathematics, 2022, 3826702, 2022. https://doi.org/10.1155/2022/3826702

[15] Kamenko, I., Čongradac, V., Kulić, F. "A novel fuzzy logic scheme for PID controller auto-tuning", Automatika: Journal for Control, Measurement, Electronics, Computing and Communications, 63(2), pp. 365–377, 2022. https://doi.org/10.1080/00051144.2022.2043988

[16] Lee, Y.-S., Jang, D.-W. "Optimization of neural network-based self-tuning PID controllers for second order mechanical systems", Applied Sciences, 11(17), 8002, 2021. https://doi.org/10.3390/app11178002

[17] Kim, W.-Y., Seo, H.-T., Kim, S., Kim, K.-S. "Practical approach for controlling optical image stabilization system", International Journal of Control, Automation and Systems, 18(4), pp. 824–833, 2020. https://doi.org/10.1007/s12555-018-0913-0

[18] Odai, M., Atsumi, K., Otsuki, H., Arisaka, T. "Head-positioning control system using thermal actuator in hard disk drives", Microsystem Technologies, 19(9), pp. 1483–1494, 2013. https://doi.org/10.1007/s00542-013-1843-7

[19] Touil, S., Bekakra, Y., Ben Attous, D. "Influence of fuzzy power system stabilizer using different membership functions for single and multi-machine", Journal of Control, Automation and Electrical Systems, 32(5), pp. 1269–1278, 2021. https://doi.org/10.1007/s40313-021-00739-4

[20] Rohitha, P. D., Senadheera, S., Pieper, J. K. "Fully automated PID and lead/lag compensator design tool for industrial use", In: Proceedings of 2005 IEEE Conference on Control Applications, 2005. CCA 2005., Toronto, ON, Canada, 2005, pp. 1009–1014. ISBN 0-7803-9354-6 https://doi.org/10.1109/CCA.2005.1507262

[21] Tsang, K. M., Lo, W. L., Rad, A. B. "Autotuning of phase-lead controller for integrating systems", IEEE Transactions on Industrial Electronics, 47(1), pp. 203–210, 2000. https://doi.org/10.1109/41.824143

[22] Loh, A. P., Cai, X., Tan, W. W. "Auto-tuning of phase lead/lag compensators", Automatica, 40(3), pp. 423–429, 2004. https://doi.org/10.1016/j.automatica.2003.10.009

[23] Senadheera, R. S., Pieper, J. K. "Synthesis of one-touch-and-go auto-tuner for practical process controllers", International Journal of Manufacturing Technology and Management, 8(1–3), pp. 226–247, 2006. https://doi.org/10.1504/IJMTM.2006.008797

[24] Nassirharand, A. "Design of self-tuning lead-lag controllers for nonlinear systems with application to mechatronics", In: 2007 European Control Conference (ECC), Kos, Greece, 2007, pp. 5827–5832. ISBN 978-3-9524173-8-6 https://doi.org/10.23919/ECC.2007.7068228

[25] Henz Mossmann, B., Alves Pereira, L. F., Gomes da Silva Jr, J. M. "Tuning of proportional-resonant controllers combined with phase-lead compensators based on the frequency response", Journal of Control, Automation and Electrical Systems, 32(4), pp. 910–926, 2021. https://doi.org/10.1007/s40313-021-00728-7

[26] Tabatabaei, M. "Parametric optimization-based design of PI controllers: application to a DC servomechanism", World Journal of Engineering, 16(3), pp. 351–356, 2019. https://doi.org/10.1108/WJE-05-2018-0178